

Influence of Annealing Temperature on Recrystallization Texture and Formability of Extra-deep Drawing Steel for Enameling

Zhimin Zhang^{1a}, Zaiwang Liu^{1b}, Xueqi Huang^{1c}, Yongqiang Xue^{2d} and Libin Yang^{2e}

¹Shougang Group Co.,Ltd. Research Institute of Technology, Beijing, China

²Shougang Jingtang United Iron & Steel Co.,Ltd, Tangshan, China

Keywords: Extra-deep drawing steel for enamelling, Annealing temperature, Recrystallization texture, precipitated phase.

Abstract: Extra-deep drawing steel sheets for enameling were annealed at different temperatures. Microstructure, precipitated particles and recrystallization texture of annealed steel were observed. Mechanical properties of annealed steel were measured. Results show that recrystallization textures of annealed steel mainly distribute along γ orientation line. Main recrystallization textures of annealed steel are $\{111\}\langle 110\rangle$ and $\{111\}\langle 112\rangle$. r value increases with the increase of annealing temperature due to higher intensity of textures $\{111\}\langle 110\rangle$ and $\{111\}\langle 112\rangle$ obtained at higher temperature. With increase of annealing temperature intensity of texture $\{111\}\langle 110\rangle$ increases obviously whereas intensity of texture $\{111\}\langle 112\rangle$ shows only a small increase. Because pinning effect of TiC particles on grains with texture $\{111\}\langle 110\rangle$ is much stronger than on grains with texture $\{111\}\langle 112\rangle$. Coarsening of TiC particles is a necessary condition for full development of texture $\{111\}\langle 110\rangle$ in annealing process. It is also an important factor to obtain excellent formability for steel sheet.

1 INTRODUCTION

Cold rolled steel sheets for enameling have some particular characteristics: good appearance, high abrasion resistance, strong corrosion resistance and excellent resistance to high temperature. So they are widely used in industry of home appliances, metallurgy, chemistry and building [1]. Extra-deep drawing steel for enameling is a special steel with excellent formability and enamel property [2]. It is a kind of ultra-low carbon steel. It has high elongation, n value and r value. So it is suitable to make some products with complex shape and strict enameling process, such as bathtub, electric oven, gas cooker, decoration panel for building and so on.

Fish-scaling resistance is necessary for enameling steel [3]. Fish-scaling resistance of enameling steel is studied in many references [3-6]. Formability and recrystallization texture are also necessary for extra-deep drawing steel for enameling. The excellent deep drawing property of steel is closely related to γ texture ($\langle 111\rangle//ND$) [7]. The greater the number of grains with lattice plane $\{111\}$ parallel to rolled surface means higher r value

and better formability [8]. Microstructure, precipitated phase, recrystallization texture and formability of extra-deep drawing steel for enameling annealed at different temperatures were observed or measured in this work in order to study the relation between formability and recrystallization texture.

2 MATERIALS AND METHODS

The experimental material is cold rolled steel sheets which can make into extra-deep drawing steel sheets for enameling by annealing process. Chemical composition of experimental steel is shown in Table 1.

Table 1: Chemical composition of experimental steel (mass fraction, %).

C	Si	Mn	P	S	Al	Ti
0.005	0.04	0.17	0.01	0.01	0.05	0.05

The experimental steel sheets were annealed at 750, 790 and 830 °C respectively. Annealing method

was continuous annealing. Tested samples were cut out from annealed steel sheets for optical microscope (OM), transmission electron microscope (TEM), texture and mechanical property experiment. All samples were cut out at 1/4 sheet width position. Size of samples for OM and TEM experiment was 10mm×10mm×0.6mm. Microstructures were observed by LEXT3100 OM and precipitates were observed by JEM-2100F(HR) TEM. Size of samples for texture was 20mm×15mm×0.6mm. Recrystallization texture was measured by X-Ray Diffractometer. Mechanical property experiment was carried out by Instron tensile testing machine following national standard GB/T 228.1-2010. Gauge length of sample for tensile testing was 50mm. Tensile direction was perpendicular to rolling direction.

3 RESULTS AND ANALYSIS

3.1 Microstructure and Precipitated Phase

Microstructures of steel annealed at different temperatures are shown in Figure 1. It can be seen from Figure 1 that microstructures of steel annealed above 750 °C are fully recrystallized. Microstructures of annealed steel consist of ferrite and some fine precipitated particles. Size of ferrite grains increases during annealing process. The higher annealing temperature, the bigger size of ferrite grains, shows Figure 1. Average size of ferrite grains for steel annealed at 750, 790 and 830 °C is 15.2, 17.8 and 18.5 μm respectively. Precipitated particles in ferrite matrix of steel annealed at different temperature observed by TEM are shown in Figure 2.

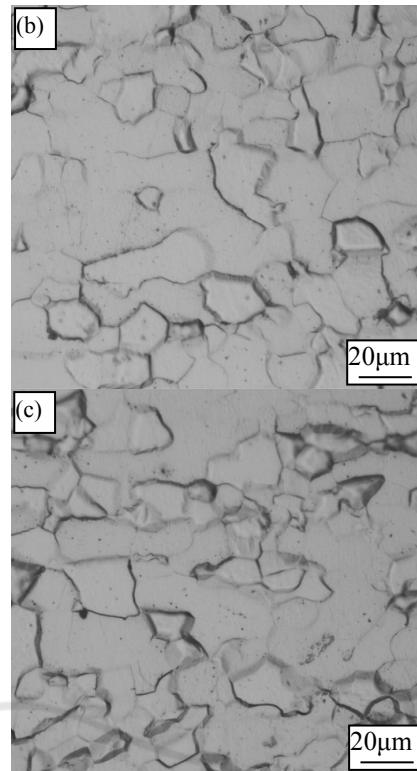
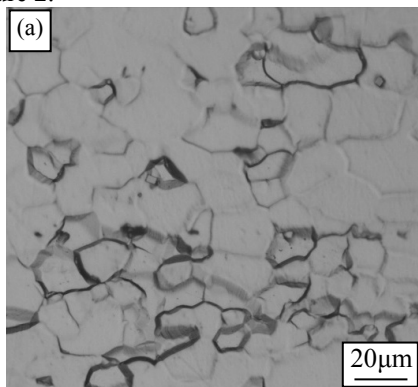
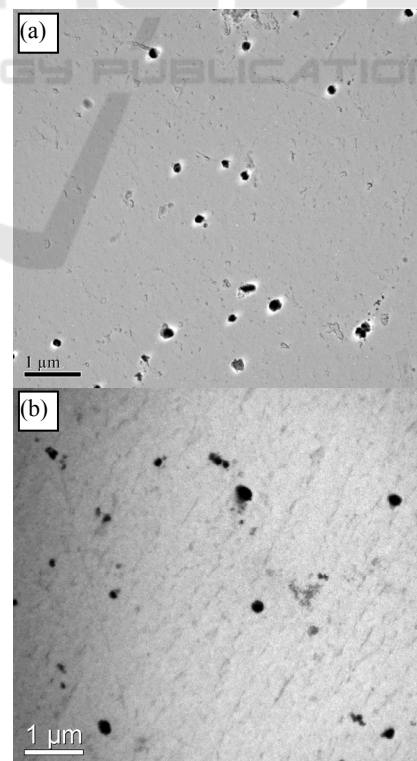


Figure 1: Microstructure of steel annealed at different temperatures (a) 750 °C; (b) 790 °C; (c) 830 °C.



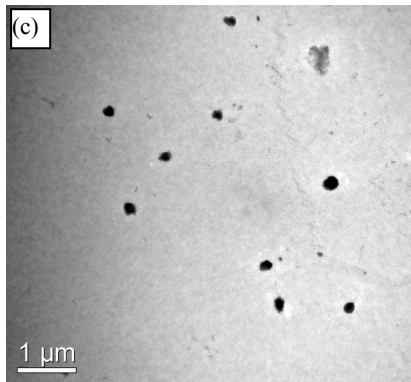


Figure 2: Precipitated particles in steel annealed at different temperatures (a) 750 °C; (b) 790 °C; (c) 830 °C.

It can be seen from Figure 2 that size of precipitated particles increases during annealing process. The higher annealing temperature, the bigger size of precipitated particles, shows Figure 2. Average size of precipitated particles in steel annealed at 750, 790 and 830 °C is 101.2, 118.0 and 148.9 nm respectively. Precipitated particle was identified as TiC by indexing corresponding diffraction spot, as shown in Figure 3.

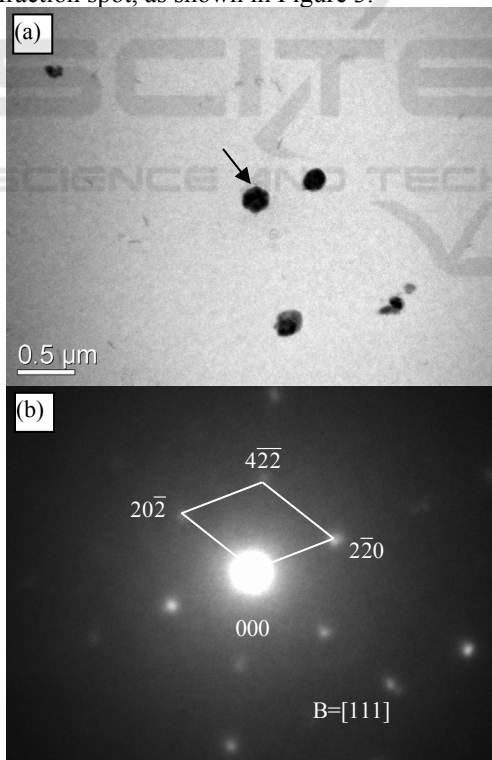


Figure 3: Precipitated particles in steel annealed at 830 °C (a) and diffraction spot (b).

3.2 Recrystallization Texture

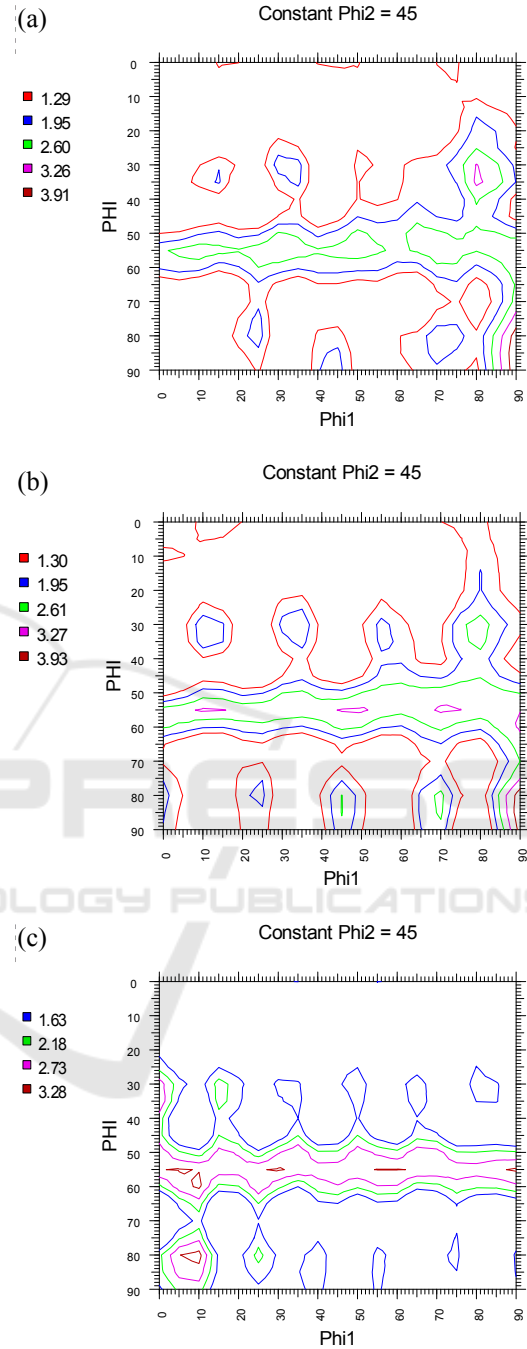


Figure 4: Orientation distribution function sections (ODFs) in $\phi_2=45^\circ$ of steel annealed at different temperatures (a) 750 °C; (b) 790 °C; (c) 830 °C.

Orientation distribution function sections (ODFs) in $\phi_2=45^\circ$ of steel annealed at different temperatures are shown in Figure 4. It can be seen from Figure 4 that recrystallization textures of annealed steel mainly distribute along γ orientation line. When

steel is annealed at 750 °C, intensity peak is 3.91 and the corresponding texture is $\{110\}\langle 001\rangle$, secondary intensity peak is 2.60 and the corresponding texture is $\{111\}\langle 112\rangle$. When steel is annealed at 790 °C, intensity peak is 3.93 and the corresponding texture is $\{110\}\langle 001\rangle$, secondary intensity peak is 3.27 and the corresponding texture is $\{111\}\langle 112\rangle$. When steel is annealed at 830 °C, intensity peak is 3.28 and the corresponding texture is $\{111\}\langle 110\rangle$, secondary intensity peak is 3.28 and the corresponding texture is $\{111\}\langle 112\rangle$. Higher intensity of recrystallization texture means higher volume fraction of grains with corresponding recrystallization texture.

Orientation densities on α orientation line of steel annealed at different temperatures are shown in Figure 5. It can be seen from Figure 5 that intensity peak is 2.5 and the corresponding texture is $\{111\}\langle 110\rangle$ when steel is annealed at 750 °C, intensity peak is 2.9 and the corresponding texture is $\{111\}\langle 110\rangle$ when steel is annealed at 790 °C, intensity peak is 3.28 and the corresponding texture is $\{111\}\langle 110\rangle$ when steel is annealed at 830 °C. Intensity of texture $\{111\}\langle 110\rangle$ increases obviously with increase of annealing temperature.

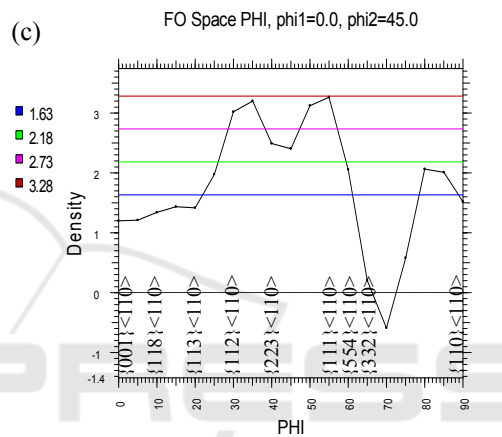
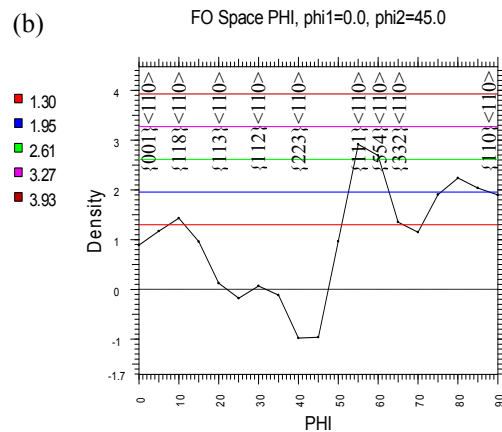
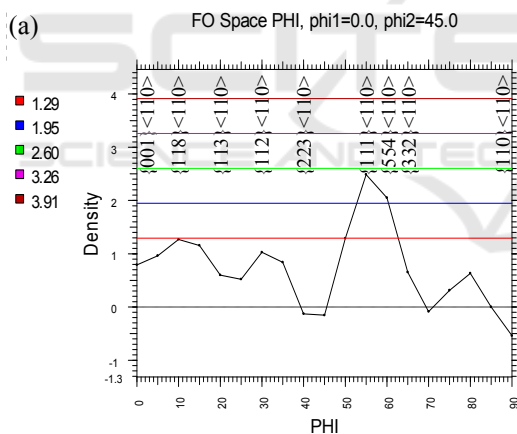
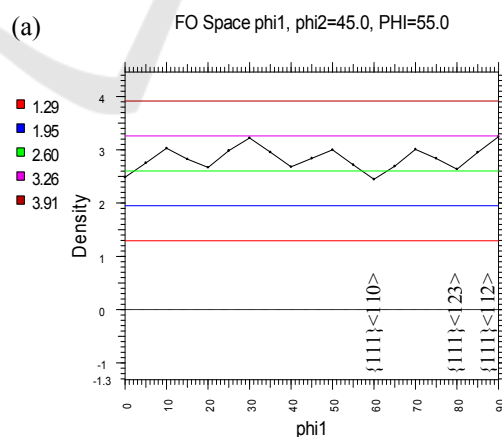


Figure 5: Orientation densities on α orientation line of steel annealed at different temperatures (a) 750 °C; (b) 790 °C; (c) 830 °C.



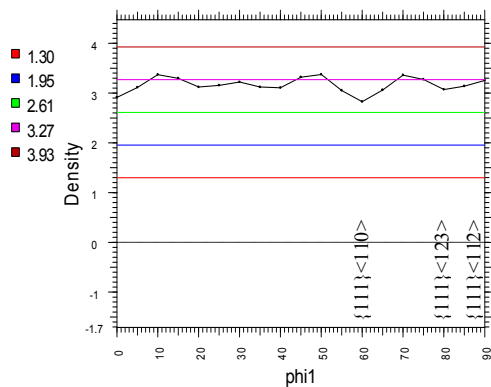
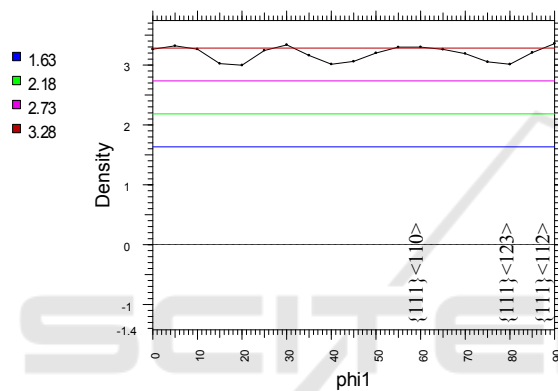
(b) FO Space ϕ_1 , $\phi_2=45.0$, $\text{PHI}=55.0$ (c) FO Space ϕ_1 , $\phi_2=45.0$, $\text{PHI}=55.0$ 

Figure 6: Orientation densities on γ orientation line of steel annealed at different temperatures (a) 750 °C; (b) 790 °C; (c) 830 °C.

Orientation densities on γ orientation line of steel annealed at different temperatures are shown in Figure 6. It can be seen from Figure 6 that when steel is annealed at 750 °C, intensity peak is 3.26 and the corresponding texture is $\{111\}\langle 110\rangle$. When steel is annealed at 790 °C, intensity peak is 3.4 and the corresponding texture is between $\{111\}\langle 110\rangle$ and $\{111\}\langle 123\rangle$, secondary intensity peak is 3.27 and the corresponding texture is $\{111\}\langle 112\rangle$. When steel is annealed at 830 °C, intensity peak is 3.28 and the corresponding texture is $\{111\}\langle 112\rangle$.

3.3 Mechanical Properties

Table 2: Mechanical properties of steel annealed at different temperatures.

Annealing temperature	$R_{p0.2}$ (MPa)	R_m (MPa)	A_{50} (%)	n	r
750 °C	120	294	46.0	0.29	2.30
790 °C	110	288	49	0.30	2.35

830 °C	105	295	47.5	0.31	2.68
--------	-----	-----	------	------	------

Mechanical properties of steel annealed at different temperatures are shown in Table 2. It can be seen from Table 2 that: with increase of annealing temperature, yield strength ($R_{p0.2}$) decreases, n value and r value increases but tensile strength (R_m) has no obvious change. Formability of extra-deep drawing steel is closely related to mechanical properties, especially r value. Higher r value means better formability. r value is closely related to recrystallization texture.

4 DISCUSSION

According to Figure 5 and Figure 6, with increase of annealing temperature, intensity of texture $\{111\}\langle 110\rangle$ increases obviously whereas intensity of texture $\{111\}\langle 112\rangle$ shows only a small increase. Sizes of grain and precipitates, recrystallization texture and r value of steel annealed at different temperatures are listed in Table 3. It can be seen from Table 3 that main recrystallization textures of experimental steel are $\{111\}\langle 110\rangle$ and $\{111\}\langle 112\rangle$ which contribute to high r value. r value increases with the increase of annealing temperature due to higher intensity of textures $\{111\}\langle 110\rangle$ and $\{111\}\langle 112\rangle$ obtained at higher temperature. This indicates volume fraction of grains with texture $\{111\}\langle 110\rangle$ or texture $\{111\}\langle 112\rangle$ increases at higher annealing temperature.

Table 3: Sizes of grain and precipitated TiC, recrystallization texture and r value of steel annealed at different temperatures.

Annealing temperature (°C)	Grain size, μm	Sizes of TiC, nm	Main recrystallization texture	Density of texture	r
750	15.2	101.2	$\{111\}\langle 110\rangle$	2.5	2.30
			$\{111\}\langle 112\rangle$	3.26	
790	17.8	118	$\{111\}\langle 110\rangle$	2.9	2.35
			$\{111\}\langle 112\rangle$	3.27	
830	18.5	148.9	$\{111\}\langle 110\rangle$	3.28	2.68
			$\{111\}\langle 112\rangle$	3.28	

Recrystallization of metal includes nucleation and growth of recrystallized grains. According to Figure 1, all grains of steel annealed at 750 °C are equiaxed. So growth of recrystallized grains is only involved and nucleation of recrystallized grains is not involved when steel is annealed above 750 °C. This mechanism of secondary phases is Ostwald ripening [9]. During annealing process, volume

fraction of TiC in steel remains the same, but size of TiC particles increases and quantity of TiC particles decreases. Growth of recrystallized grains should satisfy both thermodynamic condition and kinetics condition. Kinetics condition is activity of grain boundaries. The relation between activity of grain boundaries B and diffusion coefficient of grain boundaries D is [10]:

$$B=D/RT \quad (1)$$

where R is gas constant, T is temperature. The relation between D and T is

$$D = D_0 e^{-\frac{Q}{RT}} \quad (2)$$

where D_0 is diffusion constant, Q is diffusion activation energy. Activity of grain boundaries increases with increase of temperature. Rising temperature provides power to migration of grain boundaries. Grain boundaries also receive resistance. The resistance comes from precipitated particles in steel. Resistance F per unit area of grain boundary can be described as [10]:

$$F = \frac{3\phi\gamma_b}{2r} \quad (3)$$

where ϕ is volume fraction of precipitated particles, γ_b is energy per unit area of grain boundary, r is radius of precipitated particle. It can be seen from Equation (3) that F will decrease if ϕ decreases or r increases. From Table 3 size of precipitated TiC increases with increase of annealing temperature. F should decrease with increase of annealing temperature. That is to say, pinning effect of TiC on grain boundaries weakens with increase of annealing temperature.

If pinning effect of TiC on grains with all kinds of texture is the same, growth chance of grains with every texture is similar, intensity of every texture will have no obvious change with increase of size of TiC. But pinning effects of TiC on grains with texture $\{111\}\langle 110 \rangle$ and on grains with texture $\{111\}\langle 112 \rangle$ are different in fact. From Table 3, with increase of size of TiC, intensity of texture $\{111\}\langle 110 \rangle$ increases obviously whereas intensity of texture $\{111\}\langle 112 \rangle$ shows only a small increase. It indicates pinning effect of TiC on grains with texture $\{111\}\langle 110 \rangle$ is much stronger than on grains with texture $\{111\}\langle 112 \rangle$. During annealing process TiC particles coarsen and their pinning effect on grains weakens. So intensity of texture $\{111\}\langle 110 \rangle$ and $\{111\}\langle 112 \rangle$ increases and intensity of texture

$\{111\}\langle 110 \rangle$ increases obviously. Coarsening of TiC particles is a necessary condition for full development of texture $\{111\}\langle 110 \rangle$ in annealing process. It is also an important factor to obtain excellent formability for steel sheet.

5 CONCLUSIONS

(1) Recrystallization textures of extra-deep drawing steel for enameling after annealing process mainly distribute along γ orientation line. Main recrystallization textures of annealed steel are $\{111\}\langle 110 \rangle$ and $\{111\}\langle 112 \rangle$.

(2) r value increases with the increase of annealing temperature due to higher intensity of texture $\{111\}\langle 110 \rangle$ and $\{111\}\langle 112 \rangle$ obtained at higher temperature. With increase of annealing temperature intensity of texture $\{111\}\langle 110 \rangle$ increases obviously whereas intensity of texture $\{111\}\langle 112 \rangle$ shows only a small increase. Because pinning effect of TiC particles on grains with texture $\{111\}\langle 110 \rangle$ is much stronger than on grains with texture $\{111\}\langle 112 \rangle$.

(3) In annealing process TiC particles coarsen and their pinning effect on grains weakens. Coarsening of TiC particles is a necessary condition for full development of texture $\{111\}\langle 110 \rangle$ in annealing process. It is also an important factor to obtain excellent formability for steel sheet.

REFERENCES

1. DONG Futao, DU Linxiu, LIU Xianghua, et al. Influence of continuous annealing process on microstructure and properties of boron containing enamel steel [J]. Acta Metallurgica Sinica, 2013, 49(10):1160-1168.
2. SUN Quanshe. Mechanism research and development of extra deep drawability cold-rolled sheet steel for enameling [D]. Beijing: University of Science and Technology Beijing, 2007.
3. FENG Zhimin, FU Yulan, ZHAO Keqing. Remedy for fishscale on enamel steel sheet [J]. Acta Metallurgica Sinica, 1986, 22(4):B189-B191.
4. DONG Futao, DU Linxiu, LIU Xianghua, et al. Effect of Ti(C,N) precipitation on texture evolution and fish-scale resistance of ultra-low carbon Ti-bearing enamel steel [J]. Journal of Iron and Steel Research, International, 2013, 20(4): 39-45.
5. YUAN Xiaomin, ZHANG Qingan, SUN Quanshe. Measurement of precipitates in enameled steel sheet [J]. Journal of Iron and Steel Research, 2000, 12(5): 58-60.

6. Nicholas Winzer, Oliver Rott, Richard Thiessen, et al. Hydrogen diffusion and trapping in Ti-modified advanced high strength steels [J]. *Materials & Design*, 2016, 92:450-461.
7. CHEN Weiye, TONG Weiping, ZHANG Hui, et al. Texture evolution and growth of differently sized grains in IF steel during annealing [J]. *Acta Metallurgica Sinica*, 2010, 46(9): 1055-1060.
8. QIAN Jianqing, YUAN Xinyun. Properties testing and defect analysis of deep drawing cold-rolled sheet steel [M]. Beijing: Metallurgical Industry Press, 2012, 72-73.
9. YONG Qilong, 2006. *Secondary phases in steels* Metallurgical Industry Press. Beijing.
10. SHI Deke, 1999. *Fundamentals of material science* [M]. Machine Press. Beijing.

